Artificial magnetism and left-handed media from dielectric rings and rods

2010 J. Phys.: Condens. Matter 22 025902

(http://iopscience.iop.org/0953-8984/22/2/025902)

IOP Publishing Journal of Physics: Condensed Matter

J. Phys.: Condens. Matter **22** (2010) 025902 (6pp) doi:10.1088/0953-8984/22/2/025902

Artificial magnetism and left-handed media from dielectric rings and rods

L Jelinek[1,2] **and R Marqués**[2]

[1] Department of Electromagnetic Field, Czech Technical University in Prague, 166 27-Prague, Czech Republic
[2] Departamento de Electrónica y Electromagnetismo, Universidad de Sevilla, 41012-Sevilla, Spain

E-mail: l_jelinek@us.es

Received 16 October 2009, in final form 23 November 2009
Published 14 December 2009
Online at stacks.iop.org/JPhysCM/22/025902

Abstract

It is shown that artificial magnetism with relatively large frequency bandwidth can be obtained from periodic arrangements of dielectric rings. Combined with dielectric rods, dielectric rings can provide 3D isotropic left-handed metamaterials which are an advantageous alternative to metallic split ring resonators (SRRs) and/or metallic wires when undetectability by low frequency external magnetic fields is desired. Furthermore it is shown that, unlike conventional SRRs, dielectric rings can also be combined with natural plasma-like media to obtain a left-handed metamaterial.

1. Introduction

Metamaterials, that is, artificial effective media with properties not found in Nature, such as negative magnetic permeability and/or permittivity, have recently been the subject of a big wave of scientific interest due to the unique new physical properties and promising applications (see, e.g., [1] and references therein). For the present state of the art, the most common way to artificial magnetism uses metallic rings loaded either with a lumped capacitor [2] or with a distributed capacitance [3]. This last configuration—the so called split ring resonator (SRR)—is by far the most common configuration due to its easy manufacturing by means of standard photo-etching techniques.

There can be, however, other possibilities for obtaining artificial magnetism, and, in particular, intensive research has been recently aimed at the substitution of metallic particles by purely dielectric resonators in order to reduce losses and/or minimize interactions with low frequency external magnetic fields. The overwhelming majority of these dielectric resonators are based on Mie resonances of variously shaped dielectric/plasmonic bodies such as long cylinders [4–6], cubes [7–9] and spheres [10–15].

Throughout this paper we will show that uniform dielectric rings (DRs) present unconventional LC quasi-static magnetic resonances, which can be advantageously used in the design of negative permeability effective media. It will also be shown that connected networks of dielectric rods (DRos) can be used for the design of negative permittivity media, and that a combination of the two designs provides a left-handed behavior. The advantages of these approaches over conventional designs using dynamic Mie resonances will be discussed. The paper is organized as follows. First it will be shown that high permittivity DRs present magnetic resonances that can be described using an LC quasi-static model, in a rather similar way to that for capacitively loaded rings and/or SRRs. Then, the usefulness of these resonances for the design of negative permeability effective media will be proven and discussed. The possibility of designing left-handed metamaterials by combining DRs with other elements will also be investigated. In particular, it will be shown that combinations of DRs with a network of connected DRos, similar to conventional combinations of SRRs and wires, can provide a left-handed behavior. Finally, the effective medium properties of a combination of DRs with natural plasma-like media will be analyzed.

2. The dielectric ring

To show the principle of operation of the DR, let us assume a ring of mean radius a made of a 'dielectric wire' of radius b, as sketched in figure 1(a). Let the permittivity of the ring be $\varepsilon = \varepsilon'(1 + \mathrm{i}\tan\delta)$ and let the ring be placed in a

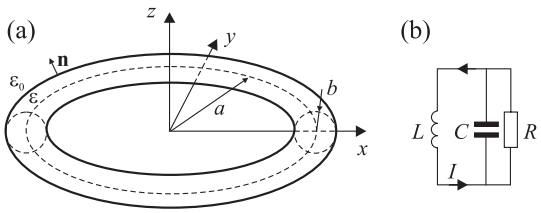

Figure 1. (a) Sketch of the proposed dielectric particle. (b) Equivalent circuit model.

homogeneous time varying magnetic field directed along the ring axis. For high enough permittivities, ε, it can be assumed that the electric field is strongly confined inside the ring due to the boundary condition $\mathbf{E}\cdot\mathbf{n} = \varepsilon_0/\varepsilon \mathbf{E}_0\cdot\mathbf{n} \approx 0$ (see figure 1(a)). Therefore, assuming a uniform distribution of the electric field inside the ring, an axial magnetic field will induce an uniform displacement current in the ring given by

$$I = -\mathrm{i}\omega\varepsilon A E_\varphi, \tag{1}$$

where $A = \pi b^2$ is the cross-section of the wire and E_φ is the angular component of the electric field, which can be determined from Faraday's law:

$$2\pi a E_\varphi = \mathrm{i}\omega(\phi^{\mathrm{int}} + \phi^{\mathrm{ext}}), \tag{2}$$

where $\phi^{\mathrm{int}} = LI$ is the internal magnetic flux due to the self-inductance of the ring and ϕ^{ext} is the external driving magnetic flux. Substituting (1) into (2) we obtain

$$\left(\frac{2\pi a}{\mathrm{i}\omega\varepsilon A} + \mathrm{i}\omega L\right) I = -\mathrm{i}\omega\phi^{\mathrm{ext}}. \tag{3}$$

In (3) the first term in the bracket can be easily recognized as the impedance $Z = (1/R - \mathrm{i}\omega C)^{-1}$ coming from the parallel combination of a capacitor C and a resistor R:

$$C = \frac{\varepsilon' A}{2\pi a}; \qquad R = \frac{2\pi a}{A\omega\varepsilon' \tan\delta} \tag{4}$$

which formally are the capacitance and the resistance of an ideal parallel plate capacitor of plate surface equal to the wire cross-section and the distance between plates equal to the circumference of the ring. Equation (3) leads to the equivalent circuit shown in figure 1(b), where L can be evaluated as [16]

$$L = \mu_0 a[\ln(8a/b) - 7/4]. \tag{5}$$

Equation (3) can also be used to calculate the axial magnetic polarizability of the particle:

$$\alpha_{zz}^{mm} = \frac{(1 + \mathrm{i}\tan\delta)(\pi a^2)^2/L}{(\frac{\omega_0^2}{\omega^2} - 1 - \mathrm{i}\tan\delta)}, \tag{6}$$

where $\omega_0 = 1/\sqrt{LC}$. Therefore, the electrical size of the DR at resonance is

$$\frac{2a}{\lambda_0} = \frac{\sqrt{2}}{\pi}\frac{a/b}{\sqrt{[\ln(8a/b) - 7/4]}}\frac{1}{\sqrt{\varepsilon_{\mathrm{r}}'}}. \tag{7}$$

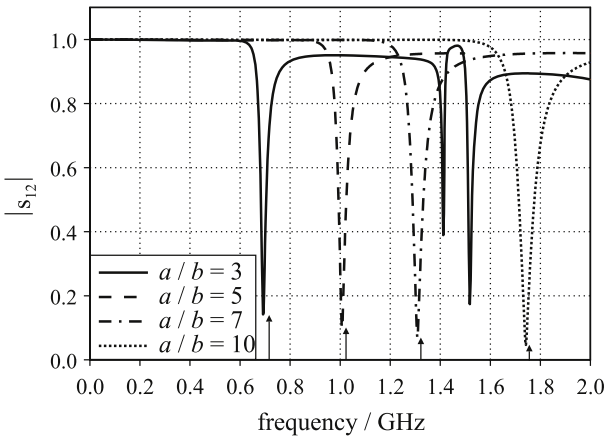

Figure 2. Transmittances through a square TEM waveguide of lateral size $4a$ loaded with a dielectric ring resonator with $a = 15$ mm and $\epsilon_{\mathrm{r}} = 250$ for several a/b ratios. Curves come from numerical simulations. Arrows show the resonances predicted from the reported analytical model.

From (7) it follows that in order to reduce the electrical size of the DR, high permittivity dielectrics and/or low a/b ratios must be used. Since losses should increase with permittivity, it will be advantageous to use a/b ratios that are as small as possible. Assuming $a/b = 3$, we can see that in order to achieve an electrical size $a/\lambda_0 \sim 0.1$, the real part of the ring permittivity must be $\varepsilon \sim 100\varepsilon_0$, which is a quite achievable value at microwave and THz frequencies.

To check our analytical results, several DRs with different a/b ratios have been designed and simulated using CST Microwave Studio[3]. To obtain the resonance frequency and the field distribution at resonance, an ideal square TEM waveguide (with upper and lower perfect electric conducting walls, and lateral perfect magnetic conducting walls) was loaded with a dielectric ring, and the scattering parameters were calculated. The dielectric ring was placed at the center of the TEM waveguide, with its axis along the incident magnetic field direction. With this configuration, any resonance of the dielectric ring will appear as a sharp dip in the transmission coefficient. Figure 2 shows the simulated transmission coefficients and the resonances predicted by our analytical model for several values of the a/b ratio. A very good agreement can be observed, even for a/b ratios as small as $a/b = 3$. The higher order DR resonances which appear in the figure for the smaller a/b ratio are electric resonances, whose description is outside the scope of our model. The electric field simulations shown in figure 3 also confirm the hypothesis underlying the model, particularly the uniformity of the field along the ring. Besides the dielectric nature, a noticeable advantage of the proposed DR is that it allows for the design of unit cells exhibiting full cubic symmetry ($\mathrm{O_h}$ group symmetry), thus being able to form isotropic metamaterials [17]. Such an

[3] In the case of figures 2, 3, 9 the time domain solver (FDTD) has been used. The structure was fed by TEM waveguide ports. In the case of figures 7 and 8 the eigensolver with the Jacobi–Davidson computation scheme has been used. In both simulations the PEC or PMC walls have been used on allowed symmetry planes. The mesh used globally 20 mesh cells per wavelength and local refinement in the rings/wires with 15 mesh cells along the wire diameter.

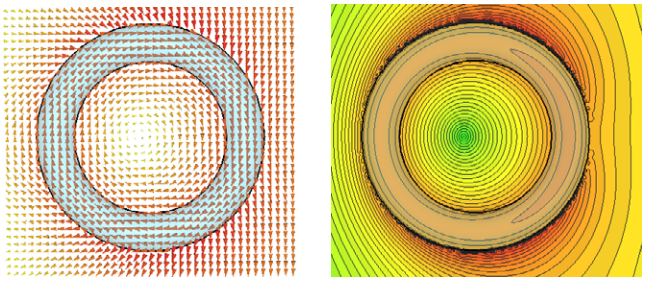

Figure 3. Vector and contour plot of the electric field intensity in the vicinity of the dielectric ring resonance. The incident wave is the TEM waveguide mode with the magnetic field along the axis of the ring. The contour plot shows the absolute value of the field. The ring and waveguide parameters are the same as in figure 2.

(This figure is in colour only in the electronic version)

isotropic composite, whose unit cell is shown in the inset of figure 4, can be described using the homogenization model developed in [18, equation 13] combined with the magnetic polarizability (6), which leads to the local effective magnetic permeability

$$\mu/\mu_0 = 1 + \frac{\frac{\alpha_0}{p^3}}{\frac{\omega_{0c}^2}{\omega^2} - 1 - \frac{2M_a}{L} - \frac{4M_c}{L} - \frac{\alpha_0}{3p^3}}, \qquad (8)$$

where p is the lattice constant, $\omega_{0c}^2 = \omega_0^2/(1 + i\tan\delta)$, $\alpha_0 = \mu_0(\pi a^2)^2/L$ and M_a and M_c are the mutual inductances of the closest rings of the same orientation, placed in the coplanar and the axial directions, respectively. Equation (8) is depicted in figure 4. The theoretical relative bandwidth of the negative permeability region shown in figure 4 is about 10%, whereas the simulated bandwidth is about 14% (see figure 7, below), more than one order of magnitude larger than in other previous designs of dielectric negative permeability media using Mie resonances of dielectric rods, cubes or spheres in free space [4–15]. The reason for this enhanced bandwidth may be the strong confinement of current in the periphery of the DR, which results in a stronger magnetic moment.

3. Dielectric rods

The high symmetry of DRs also suggests the possibility of designing a 3D isotropic left-handed medium by combining them with a connected network of metallic wires [19]. Actually, the field confinement concept underlying DR theory can also be applied in the design of a fully dielectric and isotropic left-handed metamaterial by substituting the metallic wires with dielectric rods (DRos). To keep the explanation as simple as possible, we will stick to the parallel plate waveguide model of the cubic wire medium [1, section 2.2.2]. In the framework of this model, the unit cell of such a medium is equivalent to the circuit depicted in figure 5, where $L/p = \mu_0$ is the per unit length inductance of 'vacuum', $C/p = \varepsilon$ is the per unit length capacitance of 'vacuum', Z_w is the impedance of a wire section of length p, and p is the lattice constant. In a metallic wire medium the wire exhibits an inductance that can

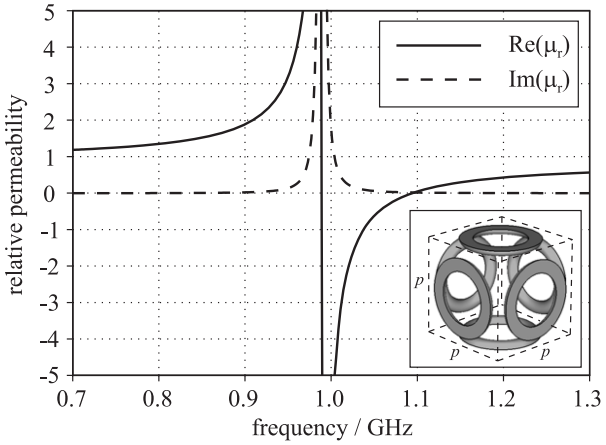

Figure 4. Effective permeability of an isotropic magnetic medium composed of DRs. The geometrical ring parameters are $a = 15$ mm and $a/b = 5$. The material is a commercially available dielectric, denoted as K-250, from TCI Ceramics, with $\epsilon_r = 250$ and $\tan\delta = 0.005$. The lattice constant is 45 mm.

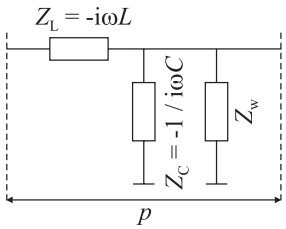

Figure 5. Equivalent circuit model of the unit cell of the connected wire medium with a cubic lattice of periodicity p.

be approximated as [19]

$$Z_w = \frac{-i\omega\mu_0 p}{2\pi}\left[\ln\left(\frac{p}{2\pi r_w}\right) + 0.5275\right], \qquad (9)$$

where r_w is the wire radius. However, as shown at the beginning of this paper, if the wires are substituted by high permittivity DRos, they also exhibit an additional capacitance and resistance (4) which result in the impedance

$$Z = \frac{-p}{i\omega\varepsilon\pi r_w^2} \qquad (10)$$

which must be added to the impedance (9). Now, the resulting effective permittivity is

$$\varepsilon_{rw} = 1 - \frac{1}{\frac{\omega^2}{\omega_p^2} - \frac{(p/r_w)^2}{\varepsilon_r\pi}}, \qquad (11)$$

where

$$\omega_p^2 = \frac{1}{\frac{\varepsilon_0\mu_0 p^2}{2\pi}\left[\ln\left(\frac{p}{2\pi r_w}\right) + 0.5275\right]} \qquad (12)$$

is the plasma frequency of the ordinary metallic wire medium. From (11) it can be seen that the presence of the additional wire capacitance shifts the resonance of the metallic wire medium from zero frequency to the higher frequency $\omega_r = pw_p/(r_w\sqrt{\epsilon_r\pi})$. The permittivity (11) is plotted in figure 6 for some realistic structural parameters.

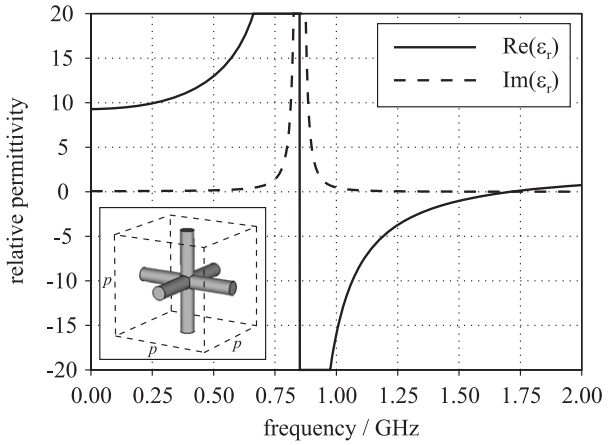

Figure 6. Effective permittivity of a connected dielectric wire medium. The geometrical parameters are $p = 45$ mm and $r_w = p/15$. The material is commercially available dielectric $SrTiO_3$ with $\epsilon_r = 500$ and $\tan\delta = 0.01$. The unit cell is shown in the inset.

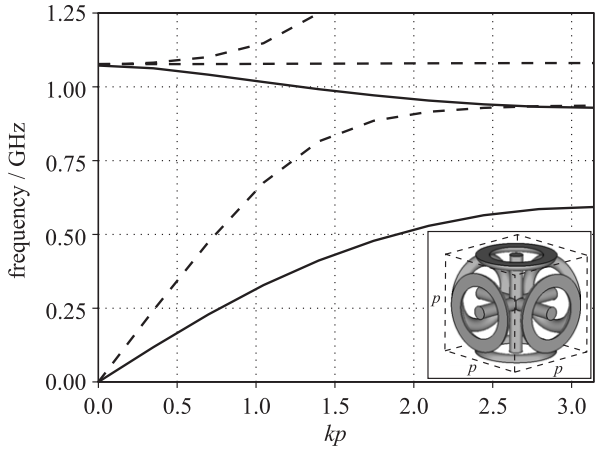

Figure 7. The band diagram of the DR + DRo medium (solid lines) with the unit cell shown in the inset and the band diagram of the DR medium alone (dashed lines). The structural parameters are the same as in figures 4 and 6; however the losses were omitted in the band-structure calculation. Note that the flat longitudinal mode in the DR band diagram will also appear in the combined structure, but has been omitted to retain the clarity of the figure.

4. The combined ring and rod medium

By combining the DR and DRo media of figures 4 and 6, the isotropic DR + DRo medium with the unit cell depicted in the inset of figure 7 is obtained. The band diagram along the Γ–X direction of this medium calculated using CST Microwave Studio is shown in figure 7, along with the band diagram for the DR medium only (losses were omitted in this calculation). A backward-wave pass band with a relative bandwidth of about 14% can be clearly observed for the DR + DRo medium. This pass band appears quite approximately at the negative permeability frequency band of the DR medium shown in figure 4. The forward pass band for the DR + DRo medium located at lower frequencies coincides almost exactly with a similar pass band for the DRo medium alone, which corresponds to the region of positive dielectric permittivity below the resonance frequency ω_r. The small numerical discrepancies in the location of the pass bands and stop bands between figures 7, 4 and 6 can be attributed to the effect of spatial dispersion, not considered in our analytical model. It should be mentioned, however, that these effects could be included in the model using the general formalism developed in [18].

5. Dielectric rings in a dielectric background

An interesting property of DRs is, that, in principle, the reported expression for capacitance (4), as well as for the magnetic polarizability (6), and the results for the magnetic permeability, are independent of the characteristics of the host medium. Increasing the permittivity of the host medium however implies a smaller jump of the dielectric constant across the ring interface, and therefore a weaker field confinement, a feature that may affect the results in practice. On the other hand, as suggested in [11], the introduction of a permittivity background can lead to increased bandwidth of the negative permeability region, making such trials worthwhile. In order to test this hypothesis we have introduced the DR

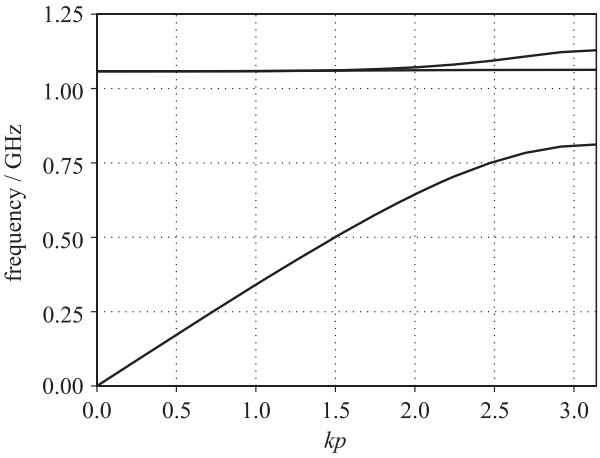

Figure 8. Band diagram of the DR medium immersed in the host material with permittivity $\varepsilon = 5\varepsilon_0$. The structural parameters are equal to those of figure 7.

lattice into the host medium with $\varepsilon = 5\varepsilon_0$ and calculated the band diagram using CST Microwave Studio. The result is depicted in figure 8. As can be observed, the material still exhibits the expected stop band at around 1 GHz and indeed its fractional bandwidth increased to approximately 27%. Further increase in the background permittivity (the value of $12\varepsilon_0$ has been tested) starts to change the band structure considerably, revealing for example a left-handed pass band in the region of previous stop band. The reason for such unexpected features can however be easily explained. Although the high permittivity background does not greatly affect the ring capacitance, it considerably enlarges the electrical size of unit cell (with respect to the wavelength of the host) and we are thus in the realm of photonic crystals rather than of homogenizable media. This analysis thus shows that the addition of a positive dielectric background can enlarge the negative permeability

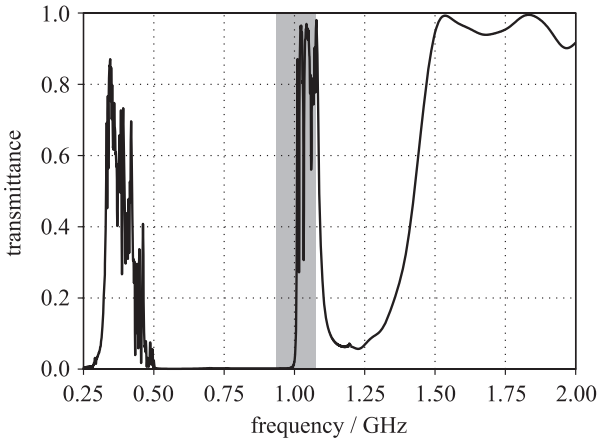

Figure 9. Transmittance through a five unit cells thick slab of DRs combined with homogeneous plasma. The plasma frequency has been set to $\omega_p = 2\pi 10^9\sqrt{2}s^{-1}$ and the collision frequency to $f_c = \omega_p/1000$. The gray-shaded area shows the region of the stop band in figure 7 arising from negative permeability. The structural parameters are the same as for figure 4.

bandwidth. However, unless the electrical size of the DR is very small, the presence of the host dielectric may lead to strong spatial dispersion or even prevent any attempt at homogenization.

The use of a low permittivity background also raises the question of whether negative permittivity can be used. In this case however another issue may appear. It is well known [20, 21, 1] that mixing two composites of negative permittivity and permeability does not ensure a left-handed behavior. In particular, an array of SRRs immersed in a homogeneous negative permittivity medium does not provide a left-handed metamaterial, because the capacitance distributed along the SRR becomes negative (that is, in fact inductive) due to the negative permittivity of the host medium [1]. Fortunately, as mentioned in the previous paragraph, the capacity of the DR should be independent of the surrounding medium. In order to further study this property of DR composites, the transmittance through a five unit cells thick slab of the DR medium, shown in figure 4, immersed in a plasma-like medium of permittivity $\varepsilon/\varepsilon_0 = 1 - \omega_p^2/(\omega(\omega - \mathrm{i}f_c))$, has been computed using CST Microwave Studio. The result is shown in figure 9.

A clear pass band in the frequency band of negative permeability of figure 4 can be observed, in agreement with the above hypothesis. Apart from this left-handed band, the structure also exhibits a right-handed pass band at lower frequencies, which results from the plasmonic resonances supported by the ring for high values of the negative permittivity of the host medium. The ripples observed in both pass bands are Fabry–Perot resonances due to the finite width of the sample. The above results for the DR furthermore suggest that also previously proposed dielectric metamaterials based on magnetic Mie resonances would provide left-handed media when immersed in a low value negative permittivity medium.

Apart from in gaseous hot plasmas, low valued negative permittivity is present in metals and in semiconductors near its plasma frequency. The plasma frequency of metals is beyond the optical range, where achieving the large permittivities needed for the proposed DR designs seems almost impossible. However, some semiconductors such as InSb [22], and others, present plasma frequencies and relatively low losses in the terahertz range, where the high dielectric constants needed for DR media design can be easily achieved. Therefore, a semiconductor matrix with DR inclusions seems to be a promising structure for left-handed media design at THz frequencies.

6. Conclusions

It has been shown that a high permittivity DR can resonate at microwave and terahertz frequencies, providing strong artificial magnetism with a frequency band of effective negative permeability one order of magnitude larger than for other previously proposed dielectric designs. By combining these DRs with DRos or with a plasma-like host medium, a left-handed behavior can be achieved. Combinations of DRs with DRos may be useful for the design of left-handed metamaterials when interactions with external low frequency magnetic fields should be minimized. A composite made of DR inclusions in a host semiconducting media near its plasma frequency appears to be a promising alternative for the design of left-handed media at terahertz frequencies. Lastly, it is also worth mentioning that the use of ferroelectrics in DRs or DRos can lead to significant tunability of the above proposed systems.

Acknowledgments

This work was supported by the Spanish Ministerio de Educación y Ciencia and European Union FEDER funds (projects TEC2007-65376, TEC2007-68013-C02-01, and CSD2008-00066), and by Junta de Andalucí a (project TIC-253). L Jelinek is also grateful for the support of the Czech Grant Agency (project No. 102/09/0314).

References

[1] Marqués R, Martín F and Sorolla M 2007 *Metamaterials with Negative Parameters: Theory and Microwave Applications* (New York: Wiley)
[2] Schelkunoff S A and Friis H T 1952 *Antennas: Theory and Practice* (New York: Wiley)
[3] Pendry J B, Holden A J, Robbins D J and Stewart W J 1999 *IEEE Trans. Microw. Theory Tech.* **47** 2075
[4] O'Brien S and Pendry J B 2002 *J. Phys.: Condens. Matter* **14** 4035
[5] Huang K C, Povinelli M L and Joannopoulos J D 2004 *Appl. Phys. Lett.* **85** 543
[6] Schuller J A, Zia R, Taubner T and Brongersma M L 2007 *Phys. Rev. Lett.* **99** 107401
[7] Zhao Q, Kang L, Du B, Zhao H, Xie Q, Huang X, Li B, Zhou J and Li L 2008 *Phys. Rev. Lett.* **101** 027402
[8] Zhao Q, Du B, Kang L, Zhao H, Xie Q, Li B, Zhang X, Zhou J, Li L and Meng Y 2008 *Appl. Phys. Lett.* **92** 051106
[9] Popa B and Cummer S A 2008 *Phys. Rev. Lett.* **100** 207401
[10] Holloway C L, Kuester E F, Baker-Jarvis J and Kabos P 2003 *IEEE Trans. Antennas Propag.* **51** 2596

[11] Yannopapas V and Moroz A 2005 *J. Phys.: Condens. Matter* **17** 3717
[12] Wheeler M S, Aitchison J S and Mojahedi M 2005 *Phys. Rev.* B **72** 193103
[13] Vendik I, Vendik O and Odit M 2006 *Microw. Opt. Technol. Lett.* **48** 2553
[14] Yannopapas V and Vitanov N V 2006 *Phys. Rev.* B **74** 193304
[15] Yannopapas V 2007 *Phys. Rev.* B **75** 035112
[16] Landau L D, Lifshitz E M and Pitaevskii L P 1984 *Electrodynamics of Continuous Media* 2nd edn (Oxford: Pergamon)
[17] Baena J D, Jelinek L and Marqués R 2007 *Phys. Rev.* B **76** 245115
[18] Baena J D, Jelinek L, Marqués R and Silveirinha M 2008 *Phys. Rev.* A **78** 013842
[19] Silveirinha M and Fernandes C A 2005 *IEEE Trans. Microw. Theory Tech.* **53** 1418
[20] Pokrovsky A L and Efros A L 2002 *Phys. Rev. Lett.* **89** 093901
[21] Marqués R and Smith D R 2004 *Phys. Rev. Lett.* **92** 059401
[22] Rivas J G, Janke C, Bolivar P H and Kurz H 2005 *Opt. Express* **13** 847